On the changing role of the stratosphere on the tropospheric ozone budget: 1979-2010

P.T. Griffiths[1,2], J. Keeble[1,2], Y.M. Shin[1], N.L. Abraham[1,2], A.T. Archibald[1,2] and J.A. Pyle[1,2]

[1]Chemistry Dept, Cambridge University, Lensfield Road, Cambridge, U.K.

[2]National Centre for Atmospheric Science, Cambridge University, U.K.

Corresponding author: Paul Griffiths (paul.griffiths@ncas.ac.uk)

Abstract

We study the evolution of tropospheric ozone over the period 1979-2010 using a chemistry-climate model employing a stratosphere-troposphere chemistry scheme. By running with specified dynamics, the key feedback of composition on meteorology is suppressed, isolating the chemical response. By using historical forcings and emissions, interactions between processes are realistically represented. We use the model to assess how the ozone responds over time and to investigate model responses and trends. We find that the CFC-driven decrease in stratospheric ozone plays a significant role in the tropospheric ozone burden. Over the period 1979-1994, the decline in transport of ozone from the stratosphere, partially offsets an emissions-driven increase in tropospheric ozone production. From 1994-2010, despite a levelling off in emissions increased stratosphere-to-troposphere transport of ozone drives a small increase in the tropospheric ozone burden. These results have implications for the impact of future stratospheric ozone recovery on air quality and radiative forcing.

Plain language summary

We use a modelling approach to study the effect of stratospheric ozone depletion on the composition of the troposphere. We focus on the period 1979-2010 and use a chemistry-climate model employing historical emissions, climate forcing and meteorology. Our model has a good description of both stratospheric and tropospheric ozone chemistry and allows us to calculate the effect of exchange between stratosphere and troposphere. We show that stratospheric ozone depletion over the period 1979-2010 has a critical effect on tropospheric composition – with less ozone in the lower stratosphere, there is less transport to the troposphere, and this offsets an emissions-driven increase in ozone production in the troposphere. Such combined studies are important to quantify the future effects of stratospheric ozone recovery on the evolution of tropospheric composition.

Introduction

The changes in tropospheric ozone since the pre-industrial era are estimated to have resulted in an increase in radiative forcing of 0.4 W m^{-2} (Stevenson et al., 2013, Myhre et al., 2013), making tropospheric ozone the third most important anthropogenic greenhouse gas. Unlike the major greenhouse gases, carbon dioxide (CO_2) and methane (CH_4), ozone is not emitted directly, but is the result of the oxidation of VOCs in the presence of NO_x (Monks et al., 2015). The tropospheric ozone abundance is controlled by a balance of sources, including photochemical production (P_{O3}) and downward transport of ozone-rich air from the stratosphere (S_{O3}), and sinks, principally physical losses at the surface (deposition, D_{O3}) and chemical loss throughout the free troposphere (L_{O3}).

Ozone has important impacts on vegetation and human health.   In addition, ozone is important since it indirectly affects the lifetime of other greenhouse gases, particularly methane, through its role in the formation of the hydroxyl radical (OH) (Voulgarakis et al., 2013). OH and ozone also have an impact on aerosol radiative forcing, a major source of uncertainty in the climate system, as secondary aerosols such as sulfate, nitrate and secondary organic aerosol are mediated by tropospheric oxidants and play a major role in the aerosol budget and burden (Karset et al., 2018). Therefore, ozone is linked throughout the Earth system, as changes in ozone can have knock on impacts on emissions of ozone precursors through feedbacks induced by changes in temperature and the hydrological cycle (driven by the changes in aerosols and clouds and radiative forcing), which themselves will modify ozone.

Measurements of ozone on a global scale are challenging, making modelling of atmospheric composition, and accurate model treatment of ozone production and loss, critical to our understanding of this important species. The International Global Atmospheric Chemistry (IGAC) Chemistry Climate Model Initiative (Eyring et al., 2016; Morgenstern et al., 2017) provided a mechanism to coordinate multi-model simulations of the historic evolution of ozone in the troposphere and stratosphere and their future evolution out to the end of the 21st Century. Results from CCMI indicate that global mean stratospheric ozone is projected to return to 1980s levels between 2045-2059 (Dhomse et al., 2018) but that the timing of this return depends on the extent of greenhouse gas emissions. As a result of increased greenhouse gas abundances, tropical total column ozone is likely to decrease by the end of the century (Oman et al., 2010; Eyring et al., 2013; Keeble et al., 2017). Revell et al. (2018) highlight a large spread in the CCMI models tropospheric ozone columns, with a bias compared to OMI-MLS data for the year 2005 of ±14 Dobson Units (~ 50%). They go on to explore the causes of bias in tropospheric ozone in the SOCOL model through performing an extensive series of sensitivity studies highlighting a large sensitivity of the SOCOL model tropospheric column ozone to emissions of ozone precursors in the year 2000.   Abalos et al. (2019) focus on the role of changes in the stratospheric influx of ozone into the troposphere over the coming century and show that models agree that an acceleration of the stratospheric circulation driven by increases in greenhouse gas emissions will result in increased stratosphere-to-troposphere transport (STT).

While we have a good understanding of the current distribution of tropospheric ozone, owing to a large number of different measurements, our understanding of changes to the historic ozone burden and budget is less complete. The Tropospheric Ozone Assessment Report (TOAR) estimates that the tropospheric ozone burden averaged over 2010-2014 is 302 (281–318) Tg (Gaudel et al., 2018). This compares well with multi-model means (MMM) from model intercomparisons of 337±23 Tg (ACCMIP,(Young et al., 2013)) and 336±27 (+16 - 21) Tg (ACCENT,(Stevenson et al., 2006) (although we note the TOAR burden is restricted to the latitude ±60˚). What controls this burden is still under debate. The recent literature on the chemical production (P_{O3}) and loss (L_{O3}) of tropospheric ozone highlights a lack of data on the topic to make reliable assessments. P_{O3} is estimated to be much larger than the source from the stratosphere (S_{O3}) in all model simulations which have calculated this (Young et al., 2018) however there is wide-spread in the magnitude of P_{O3}. Young et al. (2018) review the spread in the tropospheric ozone budget terms for the year 2000 and highlight a factor of ~ 2 spread across each term (P_{O3}, L_{O3}, S_{O3} and D_{O3}) with S_{O3} and D_{O3} having the highest spread between models. Whilst models agree that $P_{O3}>S_{O3}$ there is less agreement historically on the sign of $P_{O3}-L_{O3}$, with some models suggesting the troposphere is a net sink for ozone.

In this study we aim to understand how the budget of tropospheric ozone has evolved over the recent historical period. Our focus is 1979-2010 and our assessment is based on the results from an updated run from the CCMI nudged dynamics refC1SD simulation (Morgenstern et al., 2017). Our aim is to quantify the impact of changes in emissions of ozone precursors (and so the chemical source of tropospheric ozone) relative to the change in influx of ozone from the stratosphere over this time period. Our paper is arranged with a description of the

93 model and simulation set up (Section 2), a summary of the results of our analysis and a discussion of their
94 impacts on our understanding (Section 3). We finish with some conclusions on how future observations may
95 enable improved understanding of the role of stratospheric ozone trends on the troposphere.

96 **Method**

97
98 Here we assess recent changes to the tropospheric ozone budget using version 7.3 of the Met Office Unified
99 Model, based on the science version HadGEM3-A configuration (Hewitt et al., 2011) coupled with the United
100 Kingdom Chemistry and Aerosol scheme, hereafter UKCA-StratTrop. The simulation follows the experimental
101 design of the IGAC/Stratosphere-troposphere Processes And their Role in Climate (SPARC) Chemistry-Climate
102 Model Initiative (CCMI) refC1SD experiment. This simulation spans 1979-2010, with emissions taken from
103 MACCity (Granier et al., 2011), and uses prescribed sea surface temperatures and sea ice from HadISST
104 (Rayner et al., 2003). Horizontal wind components (u and v) and potential temperature (θ) are nudged
105 (following (Telford et al., 2008)) to ERA-Interim Reanalysis data (Dee et al., 2011). The meteorological
106 reanalysis includes dynamical effects of stratospheric ozone depletion and increased greenhouse gas
107 concentration, both of which enhance the speed of the Brewer-Dobson circulation (Abalos et al., 2019).

109 The chemical scheme used in UKCA-StratTrop is a combination of the tropospheric (O'Connor et al., 2014) and
110 stratospheric (Morgenstern et al., 2009) schemes. By using historical emissions, sea surface temperatures and
111 meteorology we are able to accurately capture both the long-term tropospheric ozone changes (driven
112 predominantly by anthropogenic emissions) and short-term changes (e.g. those driven by ENSO, etc). Further,
113 by using a combined stratosphere-troposphere chemistry scheme, the influence of stratospheric ozone changes
114 on the tropospheric ozone budget are more accurately represented.

116 A full understanding of recent changes to the tropospheric ozone burden requires detailed analysis of the
117 tropospheric ozone budget, including quantification of the chemical production and loss fluxes, stratosphere-
118 troposphere exchange and the deposition of ozone at the surface. UKCA-StratTrop includes 85 tracers, with 83
119 involved in chemistry, 59 photolytic reactions, 199 bimolecular reactions and 25 uni- and ter-molecular
120 reactions. The chemistry employs primary emissions of 12 species and dry and wet deposition of 39 and 14
121 species. Heterogeneous reactions occurring in the troposphere on sulfate aerosols are included. As a result, the
122 model includes state-of-the-art tropospheric ozone chemistry. Dry deposition is parameterised employing a
123 resistance type model (Wesely, 1989) using the implementation described in Archibald et al. (2019), while STE
124 is calculated using an online method every chemical timestep.

126 For the monthly mean data, the tropopause height was diagnosed using the WMO thermal tropopause, and a
127 mask applied to the reaction fluxes. For this study we calculate ozone production and loss terms using sums of
128 reaction fluxes, similar to the methods used by Tilmes et al. (2016). Ozone production is calculated as the
129 reaction flux through the rate-determining reactions, namely HO_2+NO, the sum of the various RO_2+NO
130 reactions involving peroxy radicals derived from methane, ethane, propane and isoprene, and the release of
131 peroxy radicals from organic nitrate photolysis, the reactions of OH with RCO_2H, organic nitrates and PAN.
132 Ozone chemical destruction is derived from O^1D+H_2O, HO_2+O_3, $OH+O_3$, ozonolysis of alkenes, as well as
133 indirect terms including loss of the O_x reservoirs, N_2O_5, and reaction of NO_3 with VOCs. Dry deposition of O_3
134 and NO_y species, as well as wet deposition of NO_y, are also included as ozone loss.

135 Table 1: tropospheric ozone budget terms, broken down into annual mean sum fluxes. All quantities are given
136 in units of $Tg(O_3)$ per year for UKCA-StratTrop integrations for year 2000.
137

Chemical O3 production / Tg per year	4751	Chemical destruction / Tg per year	4193
P1: HO2 + NO	3185	L1: O1D + H2O	2205
P2: CH3O2 + NO	1092	L2: HO2 + O3	1356
P3: RO2 + NO	345	L3: OH + O3	518
P4: OH + RCO2H	18.9	L4: O3 + ALKENE	58.2
P5: OH + RONO2	7.8	L5: NO3 Loss	50.0

P6: OH + PAN	45.9	L6: N2O5 Loss	6.6
P7: RONO2 + hv	1.8	D1: Dry deposition O3	852
P8: JO2	55.0	D2+D3: Wet + dry deposition NOy	147
STE	451 Tg	Residual (STE)	441

From the table above, it can be seen that the residual STE of ozone, calculated from the budget as STE = $L_{O3}+D_{O3}-P_{O3}$ agrees with the diagnosed online STE of ozone to within 2%. When making budget calculations, the table shows that it is important to include the contribution from photolysis of molecular oxygen in the upper tropical troposphere, which is of the order of 10% of this residual contribution, with its inclusion closing the budget to within 2%, consistent with the findings of (Prather, 2009). The model terms compare well with (Tilmes et al., 2016) for similar CCMI refC1SD experiments of P_{O3}=4693, L_{O3}=4256 and D_{O3}=871 Tg yr^{-1} and slightly lower but within the range of the ACCMIP mean values of 4937±656. 4442±570 and 996±203 Tg yr^{-1} (Young et al., 2018). The residual STT of 441 Tg yr^{-1} is within the ACCMIP range of 535 ± 161 Tg yr^{-1} (Young et al., 2013).

In order to assess the role of recent changes to the stratospheric ozone burden on the tropospheric ozone budget, a second integration (fODS_LBC) was performed in which the lower boundary condition of all halogenated ODS was kept constant at 1979 values, but all other forcings and emissions were allowed to evolve as in the HIST experiment. Comparing fODS_LBC with the HIST simulations allows us to quantify the impacts of stratospheric ozone decreases arising from the emission of halogenated ODS on tropospheric ozone. Both simulations were nudged to the same meteorology, as this isolates the chemical effects of halogenated ODS, and keeps the mass flux between the troposphere and stratosphere constant between the two experiments, ensuring that any changes to STE are the result of stratospheric ozone burden changes.

Results and Discussion

Model performance for year 2000

Figure S1 shows a comparison of the tropospheric ozone column with OMI-MLS data, generated by applying a tropospheric mask generated from a 125 ppbv ozonopause (Gaudel et al., 2018) . The UKCA-StratTrop model accurately captures the observed seasonality, albeit with a slightly late onset of ozone in the NH and a slightly early onset in the SH. The spatial structure compares well with the satellite observations, with the largest differences occurring in the boreal summer in the extratropics. The area weighted mean TCO in UKCA-StratTrop is 28.4 DU vs the OMI mean of 35.2DU. The mean ozone value is significantly closer to the OMI/MLS mean than the configuration of the models employing UKCA used in the CCMI refC1 integrations, analysed in (Revell et al., 2018), which, in contrast to the scheme used here, used a reduced complexity tropospheric chemistry scheme that does not treat NMVOC. In that configuration, UM-UKCA showed the lowest tropospheric ozone burden of the various models, with a low bias with respect to OMI/MLS of 14.1 DU for 2005 (Figure 6 of Revell et al., 2018). For these experiments, the model bias is around 7 DU low, highlighting the importance of the chemical scheme and the role of NMVOC in tropospheric ozone production. It should be noted that the exact value of the bias also depends strongly on tropopause definition, with a lower bias generally observed when using the WMO tropopause definition. The tropospheric O$_3$ burden averaged from 60ºS to 60ºN (using 125 ppbv ozonopause) is 295 Tg for year 2000, which compares well with observational estimates of between 280 Tg and 320 Tg (Gaudel et al., 2018), over the same latitude range. The model whole troposphere burden for year 2000 is 320 Tg, which is in agreement with estimates from Young et al. (2013) of 337 ± 23 Tg. Methane is forced by a lower boundary condition that follows CCMI historical concentrations at the surface, from which we derive a tropospheric CH$_4$ burden of 5000 Tg and a lifetime with respect to oxidation by tropospheric OH of 9.0 years, in good agreement with the ACCMIP mean CH$_4$ lifetime of 9.3 +/- 0.9 years (Voulgarakis et al., 2013). The airmass-weighted tropospheric mean OH is 10.6×10^5 cm^{-3} which agrees well with ACCMIP MMM of $(11.7\pm1.0)\times10^5$ cm^{-3} (Naik et al., 2013).

Evolution of tropospheric ozone burden and budget 1979-2005

Figure 1 shows the evolution of the stratospheric and tropospheric burden for both the HIST and fODS_LBC integrations. It can be seen that in HIST there is a strong decrease in modelled stratospheric ozone over the period 1980-1995 as a result of the increased CFC concentrations in the stratosphere and accompanying ozone destruction via chlorine species . Stratospheric chlorine reaches a maximum in 1997 [Maeder et al., 2010], and in the mid 1990s the decline in stratospheric ozone burden ceases, and signs of recovery emerge over the next 10 years. Over this period, the trend in tropospheric ozone burden follows the behaviour in stratospheric ozone although less strongly and with a greater effect of interannual variability. In the fODS_LBC experiment, significantly less ozone depletion is calculated, although there is some decline as the stratospheric chlorine loading adjusts to the imposed 1979 constant lower boundary condition. This adjustment requires a period of around five years for the chlorine to be transported to high latitudes by the Brewer-Dobson circulation [Butchart, 2014]. In the HIST experiment, the trend in tropospheric ozone burden is slightly negative over the period 1980-1993, and is thereafter positive. In fODS_LBC, a different behavior is calculated, with no significant trend from 1980-1993, and a positive trend thereafter.
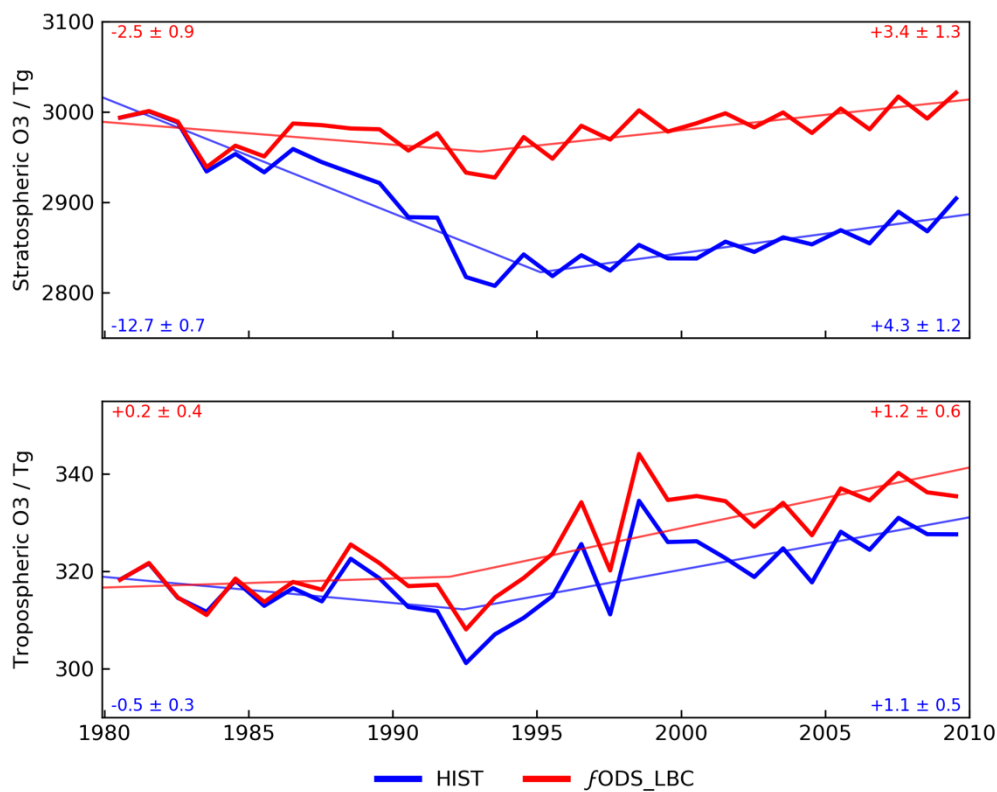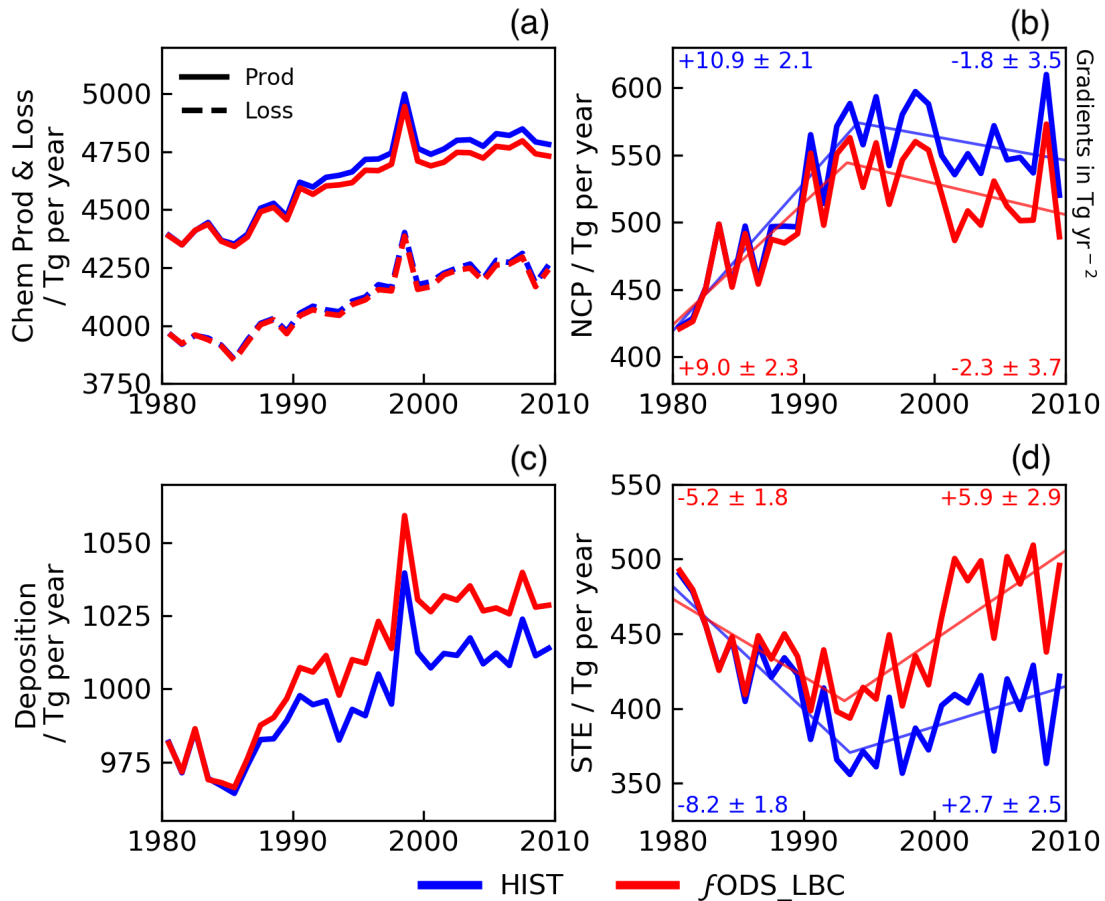

Figure 1 - Transient behaviour of annual mean stratospheric (a, upper) and tropospheric (b, lower) ozone burden.

Piecewise linear regression was used to determine the linear trends in burdens and fluxes, and these are shown in Figure 1. To fit the trends, least squares regression was used, with initial parameters determined by latin hypercube sampling, optimising using root mean square error. We find inflection points in the stratospheric burden at 1995 ($\pm$ 1 year) for the HIST run, and 1993 $\pm$ 1 at for fODS_LBC. For the troposphere, these inflection points are 1992 $\pm$ 2 for the HIST run, and 1992 $\pm$ 3 for fODS_LBC.

Discussion

The MACCity emission data (Granier et al., 2011) used for these simulations describe an increase in emissions of tropospheric ozone precursors over the period 1979-2009 which leads to enhanced chemical production, particularly at the surface in the vicinity of key emissions hotspots. Deposition, which occurs via various processes close to the surface, also increases over this period, reflecting more closely the increase in ozone production, rather than the tropospheric burden. Increases in the ozone burden do lead to an increase in OH and HO_2, particularly in the free troposphere, with concomitant increase in chemical destruction via reactions L2 and L3.

Figure 2: behavior of the fluxes controlling the tropospheric ozone burden. a: Chemical production and loss. (b): Net (P_{Ox}-L_{Ox}) chemical production. (c): Deposition of Ox and NOy. (d): Net STT of ozone. Heavy lines show the annual means, and light lines show the piecewise linear fit. In (a), the solid line shows Ox chemical production, and the dashed line shows Ox chemical loss. Captions show gradient in Tg per year^2.

Figures 2a shows the behaviour in the gross global fluxes controlling the ozone burden in both HIST and fODS_LBC. Chemical production and loss were calculated as using reactions P1-P8 and L1-L6 respectively. Figure 2b shows the difference between these terms, Net Chemical Production (NCP), while Figures 2c and 2d show deposition and STE of ozone. The deposition describes the amount of Ox deposited in wet and dry deposition, and the STE encapsulates the net transport of ozone from the stratosphere into the troposphere.

In both simulations, there is some interannual variability, with other transient features also apparent. These are associated with modes of unforced climate variability, such as ENSO, with peak and trough in ozone production occurring around strong events in the mid 1980s and in 1997. These climate events are also present in the NOx and CO emissions used in CCMI refC1SD which represent the fire emissions from these events. Spikes in ozone chemical production, loss and deposition can be seen around 1997 which reflect the strong transient increase in emissions of ozone precursors in the MACCity emissions used for these simulations, and which

240 represent the increase in biomass burning that year, particularly around SE Asia.   We examined the effect of
241 these events on the trends and find no statistically significant difference in trends when calculated when the El
242 Nino years are ignored in the analysis. Removing 1997 and 1998 from our data, resulted in the early trend
243 changing from –0.53 ± 0.34 Tg per year to –0.59 ± 0.31 Tg per year, and the later trend changing from +1.07 ±
244 0.52 Tg per year to +1.10 ± 0.48, identical within mutual uncertainty and showing that El Nino has no effect on
245 the retrieved values for the tropospheric ozone burden trend over 1979-2010. Although dynamical effects may
246 also play a part (Voulgarakis et al., 2011), there is little evidence of a transient increase in STE in these
247 integrations around this time.
248
249 Chemical production and loss of tropospheric ozone increase over the entire experiment. In HIST, over the
250 period 1979-1996, ozone production increases at a slightly faster rate than loss resulting in an increase in NCP
251 over this period. After 1996, losses increase slightly faster than production, leading to a smaller and slightly net
252 negative trend in NCP. This partially reflects the behaviour of the precursor emissions, which reach a maximum
253 around 1995 and then decline after this point. In HIST, photochemical production of ozone due to lower
254 overhead ozone and higher photolysis rates [Voulgorakis et al., 2013] than in fODS_LBC.
255
256 STE of ozone (the transport of ozone from the stratosphere into the troposphere) declines sharply from 1979-
257 1994, consistent with the decline in lower stratospheric ozone associated with the use and emission of
258 halogenated ODS, particularly the CFCs, throughout this time. From 1994-2006, modelled STE slowly
259 increases, driven in part by early signs of stratospheric ozone recovery in the mid-latitudes (e.g. (Keeble et al.,
260 2018), and stratospheric dynamical changes resulting from increased GHGs (e.g.(Butchart, 2014)). We note that
261 these two effects are not isolated, with stratospheric ozone depletion and stratospheric dynamics closely coupled
262 (e.g. Keeble et al. (2014, Polvani et al. (2018)).
263
264 In the fODS_LBC experiment, the STE term declines to a minimum in 1994, albeit at a slower rate than in
265 HIST, before increasing from 1994 to the end of the integration. The greater rate of increase in STE after 1994
266 in the fODS_LBC integration compared with HIST can be attributed to the higher stratospheric ozone burden in
267 this experiment, as the stratosphere-to-troposphere mass transport is identical between simulations. In
268 fODS_LBC NCP is lower than in HIST, particularly as the stratospheric ozone burdens in the two experiments
269 diverge and the photochemical ozone production in HIST increases.
270
271 Comparing HIST to fODS_LBC directly quantifies the chemical impacts of stratospheric ozone depletion on the
272 tropospheric ozone budget. Figure 3 shows the difference in NCP, STE and DD between the HIST simulation
273 with respect to fODS_LBC. The differences for each in the year 1980 are near zero, as the simulations start
274 from the same initial conditions. They diverge after ~5 years, consistent with the time it takes for the surface
275 ODS mixing ratios prescribed by the LBC to be transported into the polar stratosphere. After 1985, STE is
276 lower in the HIST simulation by around 75 Tg yr^{-1} between 2000-2006, reflecting the lower stratospheric ozone
277 burden, while NCP is up to 50 Tg yr^{-1} higher, reflecting the increased photochemical production of ozone.
278 Deposition of ozone follows the tropospheric burden, and so is lower in the HIST simulation by ~20 Tg yr^{-1}.
279
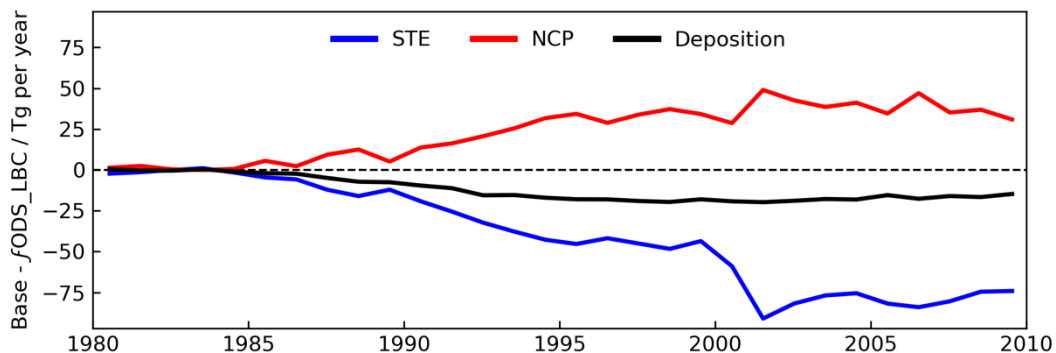
282 Figure 3: summary of HIST and fODS_LBC counterfactual experiments. The different in budget terms is
283 shown over the period of the integrations. Data are shown as HIST-fODS_LBC.
284

285 In conclusion, the HIST integration represents our best estimate of past tropospheric ozone changes as it follows
286 historical emissions and meteorology. fODS_LBC isolates the effect of stratospheric ozone decreases on the
287 tropospheric ozone budget, but also shows that the effect of circulation changes has been significant. The
288 behavior of the STE term in fODS_LBC shows that the faster Brewer-Dobson circulation and increased mass
289 flux to the troposphere are also important controls on the budget. The two experiments also show that there is
290 enhanced NCP in HIST, and that this offsets a significant decrease in ozone transport via STE, and thus
291 moderates the effect of decreased stratospheric ozone on tropospheric ozone burden.
292
293
294

Summary

296 Between 1979 and ~1994 there is an increase in NCP of tropospheric ozone in response to increases in
297 anthropogenic ozone precursors and an indirect decrease in transport to the troposphere which is the result of
298 stratospheric ozone depletion caused by halogenated ODS. These drivers are in opposition, similar in
299 magnitude, and are moderated by the change in chemical loss, resulting in a slight decrease in the tropospheric
300 ozone burden despite increases to ozone precursor emissions. From 1994 to 2006, the tropospheric ozone
301 burden has been increasing, driven by decreases to NCP again being offset by changes to STE. These drivers of
302 tropospheric ozone, which are in opposition, turn out to be of similar magnitude, leading to a near-cancelling
303 behaviour in changes to the budget terms and so a smaller change in ozone than in the P_{O3}, L_{O3} or STE terms
304 that control it.
305
306 Over the recent historical period, our study demonstrates that stratospheric ozone depletion has had a large
307 impact on tropospheric ozone. Without the resulting decrease of STE, the large increase in NCP over the period
308 1979-1994 would have increased the tropospheric ozone burden. After 1994, there is a levelling off in the
309 growth of emissions, and, coincidentally, a slight increase in STE, which together serve to increase the
310 tropospheric ozone burden.
311
312 Our study uses two complementary methods to diagnose the stratospheric input. Our chemical budget
313 diagnostics allow us to identify a residual term, which we ascribe to STE. Separately, we use dynamical
314 methods to determine the amount of stratospheric ozone transported to the troposphere. We show that these two
315 methods agree to within 2%, lending confidence to our analysis of the impact of stratospheric transport on
316 tropospheric ozone.
317
318 Our results highlight the role of the stratosphere on tropospheric composition, and the utility of whole-
319 atmosphere chemistry schemes with interactive stratospheric chemistry. Comparison with other UKCA models
320 in the CCMI project, highlights the critical role of tropospheric NMVOC chemistry in model skill. Finally, our
321 results demonstrate the importance of STT on present (Neu et al., 2014) and future tropospheric ozone (Sekiya
322 & Sudo, 2014), particularly as stratospheric ozone recovers over this century. This will be particularly
323 important in regions affected by downward transport, e.g. NH midlatitudes in springtime (Lin et al., 2015). The
324 complicating effects of circulation changes (see Polvani et al. (2018) necessitate further study at the regional
325 scale using a dynamical model with interactive chemistry to fully understand the implications of stratospheric
326 ozone recovery on tropospheric composition, radiative forcing and air quality.
327

Acknowledgements

References

Abalos, M., Polvani, L., Calvo, N., Kinnison, D., Ploeger, F., Randel, W., & Solomon, S. (2019). New Insights on the Impact of Ozone-Depleting Substances on the Brewer-Dobson Circulation. *Journal of Geophysical Research: Atmospheres*, *124*(5), 2435–2451. https://doi.org/10.1029/2018JD029301

Archibald, Alexander T., O'Connor, F. M., Abraham, N. L., Archer-Nicholls, S., Chipperfield, M. P., Dalvi, M., et al. (2019). Description and evaluation of the UKCA stratosphere-troposphere chemistry scheme (StratTrop vn 1.0) implemented in UKESM1. *Geoscientific Model Development Discussions*, 1–82. https://doi.org/10.5194/gmd-2019-246

Butchart, N. (2014). The Brewer-Dobson circulation. *Reviews of Geophysics*, *52*(2), 157–184. https://doi.org/10.1002/2013RG000448

Dee, D. P., Uppala, S. M., Simmons, A. J., Berrisford, P., Poli, P., Kobayashi, S., et al. (2011). The ERA-Interim reanalysis: configuration and performance of the data assimilation system. *Quarterly Journal of the Royal Meteorological Society*, *137*(656), 553–597. https://doi.org/10.1002/qj.828

Dhomse, S. S., Kinnison, D., Chipperfield, M. P., Salawitch, R. J., Cionni, I., Hegglin, M. I., et al. (2018). Estimates of ozone return dates from Chemistry-Climate Model Initiative simulations. *Atmospheric Chemistry and Physics*, *18*(11), 8409–8438. https://doi.org/10.5194/acp-18-8409-2018

Eyring, V., Lamarque, J.‐F., Hess, P., Arfeuille, F., Bowman, K., Chipperfield, M. P., et al. (2013). Overview of IGAC/SPARC Chemistry‐Climate Model Initiative (CCMI) community simulations in support of upcoming ozone and climate assessments, SPARC Newsletter 40.

Gaudel, A., Cooper, O. R., Ancellet, G., Barret, B., Boynard, A., Burrows, J. P., et al. (2018). Tropospheric Ozone Assessment Report: Present-day distribution and trends of tropospheric ozone relevant to climate and global atmospheric chemistry model evaluation. *Elem Sci Anth*, *6*(1), 39. https://doi.org/10.1525/elementa.291

Granier, C., Bessagnet, B., Bond, T., D'Angiola, A., Denier van der Gon, H., Frost, G. J., et al. (2011). Evolution of anthropogenic and biomass burning emissions of air pollutants at global and regional scales during the 1980–2010 period. *Climatic Change*, *109*(1), 163. https://doi.org/10.1007/s10584-011-0154-1

Griffiths, P.; Keeble, J.; Shin, Y.; Abraham, L.; Archibald, A.; Pyle, J. (2020): WCRP CCMI-1: UM-UKCA output following the CCMI refC1SD experiment protocol. Centre for Environmental Data Analysis, 2020. https://catalogue.ceda.ac.uk/uuid/549bce914f66451d838bff5c0a557b37

Hewitt, H. T., Copsey, D., Culverwell, I. D., Harris, C. M., Hill, R. S. R., Keen, A. B., et al. (2011). Design and implementation of the infrastructure of HadGEM3: the next-generation Met Office climate modelling system. *Geoscientific Model Development*, *4*(2), 223–253. https://doi.org/10.5194/gmd-4-223-2011

Karset, I. H. H., Berntsen, T. K., Storelvmo, T., Alterskjær, K., Grini, A., Olivié, D., et al. (2018). Strong impacts on aerosol indirect effects from historical oxidant changes. *Atmospheric Chemistry and Physics*, *18*(10), 7669–7690. https://doi.org/10.5194/acp-18-7669-2018

Keeble, J., Braesicke, P., Abraham, N. L., Roscoe, H. K., & Pyle, J. A. (2014). The impact of polar stratospheric ozone loss on Southern Hemisphere stratospheric circulation and climate. *Atmospheric Chemistry and Physics*, *14*(24), 13705–13717. https://doi.org/10.5194/acp-14-13705-2014

Keeble, James, Brown, H., Abraham, N. L., Harris, N. R. P., & Pyle, J. A. (2018). On ozone trend detection: using coupled chemistry–climate simulations to investigate early signs of total column ozone recovery. *Atmospheric Chemistry and Physics*, *18*(10), 7625–7637. https://doi.org/10.5194/acp-18-7625-2018

Lin, M., Fiore, A. M., Horowitz, L. W., Langford, A. O., Oltmans, S. J., Tarasick, D., & Rieder, H. E. (2015). Climate variability modulates western US ozone air quality in spring via deep stratospheric intrusions. *Nature Communications*, *6*(1). https://doi.org/10.1038/ncomms8105

Maeder, J. A., Staehelin, J., Peter, T., Brunner, D., Rieder, H. E., and Stahel, W. A.: Evidence for the effectiveness of the Montreal Protocol to protect the ozone layer, Atmos. Chem. Phys., 10, 12161– 12171, https://doi.org/10.5194/acp-10-12161-2010, 2010.

Monks, P. S., Archibald, A. T., Colette, A., Cooper, O., Coyle, M., Derwent, R., et al. (2015). Tropospheric ozone and its precursors from the urban to the global scale from air quality to short-lived climate forcer. *Atmospheric Chemistry and Physics*, *15*(15), 8889–8973. https://doi.org/10.5194/acp-15-8889-2015

Morgenstern, O., Braesicke, P., O'Connor, F. M., Bushell, A. C., Johnson, C. E., Osprey, S. M., & Pyle, J. A. (2009). Evaluation of the new UKCA climate-composition model – Part 1: The stratosphere. *Geoscientific Model Development*, *2*(1), 43–57. https://doi.org/10.5194/gmd-2-43-2009

Morgenstern, Olaf, Hegglin, M. I., Rozanov, E., O&apos;Connor, F. M., Abraham, N. L., Akiyoshi, H., et al. (2017). Review of the global models used within phase 1 of the Chemistry–Climate Model Initiative (CCMI). *Geoscientific Model Development*, *10*(2), 639–671. https://doi.org/10.5194/gmd-10-639-2017

Myhre, G., Shindell, D., Bréon, F.-M., Collins, W., Fuglestvedt, J., Huang, J., et al. (2013). Anthropogenic and Natural Radiative Forcing. In T. F. Stocker, D. Qin, G.-K. Plattner, M. Tignor, S. K. Allen, J. Boschung, et al. (Eds.), *Climate Change 2013: The Physical Science Basis. Contribution of Working Group I to the Fifth Assessment Report of the Intergovernmental Panel on Climate Change* (pp. 659–740). Cambridge, United Kingdom and New York, NY, USA: Cambridge University Press. https://doi.org/10.1017/CBO9781107415324.018

Naik, V., Voulgarakis, A., Fiore, A. M., Horowitz, L. W., Lamarque, J.-F., Lin, M., et al. (2013). Preindustrial to present-day changes in tropospheric hydroxyl radical and methane lifetime from the Atmospheric Chemistry and Climate Model Intercomparison Project (ACCMIP). *Atmospheric Chemistry and Physics*, *13*(10), 5277–5298. https://doi.org/10.5194/acp-13-5277-2013

Neu, J. L., Flury, T., Manney, G. L., Santee, M. L., Livesey, N. J., & Worden, J. (2014). Tropospheric ozone variations governed by changes in stratospheric circulation. *Nature Geoscience*, *7*(5), 340–344. https://doi.org/10.1038/ngeo2138

O'Connor, F. M., Johnson, C. E., Morgenstern, O., Abraham, N. L., Braesicke, P., Dalvi, M., et al. (2014). Evaluation of the new UKCA climate-composition model – Part 2: The Troposphere. *Geoscientific Model Development*, *7*(1), 41–91. https://doi.org/10.5194/gmd-7-41-2014

Polvani, L. M., Abalos, M., Garcia, R., Kinnison, D., & Randel, W. J. (2018). Significant Weakening of Brewer-Dobson Circulation Trends Over the 21st Century as a Consequence of the Montreal Protocol. *Geophysical Research Letters*, *45*(1), 401–409. https://doi.org/10.1002/2017GL075345

Prather, M. J. (2009). Tropospheric O3 from photolysis of O2. *Geophysical Research Letters*, *36*(3). https://doi.org/10.1029/2008GL036851

417   Rayner, N. A., Parker, D. E., Horton, E. B., Folland, C. K., Alexander, L. V., Rowell, D. P., et al. (2003). Global
418   analyses of sea surface temperature, sea ice, and night marine air temperature since the late nineteenth
419   century. *Journal of Geophysical Research: Atmospheres*, *108*(D14).
420   https://doi.org/10.1029/2002JD002670

421   Revell, L. E., Stenke, A., Tummon, F., Feinberg, A., Rozanov, E., Peter, T., et al. (2018). Tropospheric ozone in
422   CCMI models and Gaussian process emulation to understand biases in the SOCOLv3 chemistry–climate
423   model. *Atmospheric Chemistry and Physics*, *18*(21), 16155–16172. https://doi.org/10.5194/acp-18-
424   16155-2018

425   Sekiya, T., & Sudo, K. (2014). Roles of transport and chemistry processes in global ozone change on interannual
426   and multidecadal time scales. *Journal of Geophysical Research: Atmospheres*, *119*(8), 4903–4921.
427   https://doi.org/10.1002/2013JD020838

428   Stevenson, D. S., Dentener, F. J., Schultz, M. G., Ellingsen, K., Noije, T. P. C. van, Wild, O., et al. (2006).
429   Multimodel ensemble simulations of present-day and near-future tropospheric ozone. *Journal of*
430   *Geophysical Research: Atmospheres*, *111*(D8). https://doi.org/10.1029/2005JD006338

431   Telford, P. J., Braesicke, P., Morgenstern, O., & Pyle, J. A. (2008). Technical Note: Description and assessment
432   of a nudged version of the new dynamics Unified Model. *Atmospheric Chemistry and Physics*, *8*(6),
433   1701–1712. https://doi.org/10.5194/acp-8-1701-2008

434   Tilmes, S., Lamarque, J.-F., Emmons, L. K., Kinnison, D. E., Marsh, D., Garcia, R. R., et al. (2016).
435   Representation of the Community Earth System Model (CESM1) CAM4-chem within the Chemistry-
436   Climate Model Initiative (CCMI). *Geoscientific Model Development*, *9*(5), 1853–1890.
437   https://doi.org/10.5194/gmd-9-1853-2016

438   Voulgarakis, A., Hadjinicolaou, P., & Pyle, J. A. (2011). Increases in global tropospheric ozone following an El
439   Niño event: examining stratospheric ozone variability as a potential driver. *Atmospheric Science Letters*,
440   *12*(2), 228–232. https://doi.org/10.1002/asl.318

441   Voulgarakis, A., Naik, V., Lamarque, J.-F., Shindell, D. T., Young, P. J., Prather, M. J., et al. (2013). Analysis of
442   present day and future OH and methane lifetime in the ACCMIP simulations. *Atmospheric Chemistry*
443   *and Physics*, *13*(5), 2563–2587. https://doi.org/10.5194/acp-13-2563-2013

444   Voulgorakis, A., Shindell, D.T., and Faluvegi, G. Linkages between ozone-depleting substances, tropospheric
445   oxidation and aerosols, Atmos. Chem. Phys., 13, 4907–4916, 2013

446   Wesely, M. L. (1989). Parameterization of surface resistances to gaseous dry deposition in regional-scale
447   numerical models. *Atmospheric Environment (1967)*, *23*(6), 1293–1304. https://doi.org/10.1016/0004-
448   6981(89)90153-4

449   Young, P. J., Archibald, A. T., Bowman, K. W., Lamarque, J.-F., Naik, V., Stevenson, D. S., et al. (2013). Pre-
450   industrial to end 21st century projections of tropospheric ozone from the Atmospheric Chemistry and
451   Climate Model Intercomparison Project (ACCMIP). *Atmospheric Chemistry and Physics*, *13*(4), 2063–
452   2090. https://doi.org/10.5194/acp-13-2063-2013

453   Young, P. J., Naik, V., Fiore, A. M., Gaudel, A., Guo, J., Lin, M. Y., et al. (2018). Tropospheric Ozone Assessment
454   Report: Assessment of global-scale model performance for global and regional ozone distributions,
455   variability, and trends. *Elem Sci Anth*, *6*(1), 10. https://doi.org/10.1525/elementa.265

456

457